LA-UR- 98-2843

Approved for public release; distribution is unlimited.

Title: SOURCES OF FE IN EOLIAN AND SOIL DETRITUS AT YUCCA MOUNTAIN, NEVADA, USA

CONF-9706169--

Author(s): David Vaniman, EES-1
Steve Chipera, EES-1
David Bish, EES-1

Submitted to: Proceedings, 11th International Clay Conference
Ottawa, Canada, June 1997

Los Alamos
NATIONAL LABORATORY

DISCLAIMER

Sources of Fe in Eolian and Soil Detritus at Yucca Mountain, Nevada, USA

D. Vaniman, S. Chipera, and D. Bish

Geology and Geochemistry, MS D462
Los Alamos National Laboratory
Los Alamos, NM 87545

ABSTRACT

Eolian deposits and adjacent soil horizons at Exile Hill near Yucca Mountain, Nevada, provide a desert environment where the origins of exotic eolian materials can be discerned. Petrographic, chemical, X-ray diffraction, and electron microprobe data allow an assessment of Fe mineral sources. Fe-rich minerals in local rhyolitic tuff bedrock consist of distinctive biotite and amphibole phenocrysts and groundmass Mn-hematites. Although the local tuffs contain only 1% FeO, detrital components of eolian and soil deposits have ~3% FeO. Exotic minerals from distant sources provide most of the excess Fe in the surficial deposits. The exotic Fe sources are principally smectite, low-Mn hematite, low-F biotite, and high-Fe amphibole not found in local tuffs. Iron contents and the exotic Fe fraction increase with decreasing grain size, such that the clay fractions have ~5-6% FeO, almost all of which is in exotic smectites. The distant origin of these smectites is evident in their high Fe content and distinct Sc/FeO enrichment trends, which differ from the strong local Sc/FeO control defined by coarser soil detritus. Approximate "crustal average" lanthanide composition in soil and eolian smectites rule out any significant contribution of local smectite derived from tuff alteration. The eolian and soil smectites instead inherit their high Fe content from eolian biotite.

INTRODUCTION

The Fe content of eolian detritus is a matter of interest for a wide variety of studies, ranging from paleoclimatology (Balsam and Otto-Bliesner, 1995) to possible implications for the population dynamics of plankton in the world's oceans (DeBaar et al., 1995). The general emphasis on studies of eolian materials has been on quantitative chemical analysis, which provides abundant information on total Fe contents but little information on the mineral distributions of Fe. The mineralogy of Fe carriers is important for determining reactivity, solubility, provenance, and evolution of Fe in eolian materials. In this paper we link quantitative chemical analysis, by instrumental neutron activation analysis (INAA) and by electron probe microanalysis (EPM), with quantitative mineralogical analysis by X-ray diffraction (QXRD) and data from optical petrography. The site of this study is Exile Hill, a low ridge on the western flank of Yucca Mountain in Nevada, USA.

The Exile Hill locality (Fig. 1) has been studied in detail for understanding the relationships between siliceous calcretes formed along its slopes and similar calcretes that penetrate veins and fractures of the underlying rhyolitic tuffs (Vaniman et al., 1994, 1995; Taylor and Huckins, 1995). The slopes of Exile Hill range from ~6°-7° on the western flank to ~18°-20° on the eastern flank. Taylor and Huckins (1995) provide detailed descriptions of the site and summarize the development and age relations of soil A, B, and K horizons along the western alluvial slope of Exile Hill; a simplified summary of their soil stratigraphy is provided in Table 1. They recognize three major subdivisions:

an upper silty sand (Unit 1) that appears to be mostly eolian, an older silty sand to sandy silt (Unit 2), and a thick underlying series of siliceous calcretes (Unit 3). Taylor and Huckins (1995) infer a late Pleistocene to early Holocene age (~10 ka) for Unit 1 and cite U-trend ages of 38 and 55 ka for Unit 2 and U-trend ages that range from 88 to >550 ka for Unit 3.

In addition to the slope-parallel soil horizons developed in the slope-wash alluvium, faults at Exile Hill contain thick accumulations of calcite- and opal-cemented detritus with contorted or near-vertical laminar fabric. These fault fillings are similar in mineralogic and chemical composition to the 3Kmq slope-parallel calcretes listed in Table 1 (Taylor and Huckins, 1995; Vaniman et al., 1994). In this paper, data from both the slope-parallel 3Kmq deposits and from the fault fillings are treated together as "calcrete," because their mineralogic and chemical composition is indistinguishable (Vaniman et al., 1994, 1995). We have also sampled eolian materials trapped within fractures of boulders above the soil zone at the ridge crest (Fig. 1). These materials from above the soil zone are specifically referred to as eolian throughout this paper, whereas the Av and Btk materials, although apparently containing a large eolian component, are referred to by their soil unit designations.

Mineralogic and chemical analyses of the Exile Hill deposits are described in Vaniman et al. (1994) and compiled in Vaniman et al. (1995). In these reports it was noted that there is significantly more Fe in the detrital components of these soil horizons than in the underlying rhyolitic tuffs. Iron contents, reported as FeO, range from 2.8-3.3% in the Av, Btk, and 2Btj horizons, and from 2.4-6.2% in the detrital components (excluding calcite and opal diluents) of various samples from the fault-filling and slope-

parallel calcretes. In contrast, the rhyolitic tuffs at the site contain only ~1% FeO. Initial interpretations of the FeO enrichment in the soil detritus included the suggestion that deflation or slopewash may have removed lighter minerals and left the heavier Fe-bearing minerals behind (Vaniman et al., 1994); subsequent electron-probe microanalysis (EPM) identified hematite and amphibole grains in the soils that were distinctly different from those of the local tuffs (Vaniman et al., 1995). These studies left unresolved the question of how much material in these soils is foreign to the site. In particular, although it was realized that clay separates from the B horizons were different from the average detritus in their Sc/FeO systematics, it was not known whether this reflected some local aspect of clay evolution or whether this differences was carried in by eolian introduction of clays formed elsewhere. To resolve these questions, we have examined additional material representing the soil Av horizon, as well as the eolian dusts collected from fractures in surface outcrops that are higher than and isolated from the soil horizons.

METHODS

Optical petrographic analysis was performed on polished thin sections. Trace-element, Ca, Fe, Na, and K data were obtained by instrumental neutron activation analysis (INAA). The INAA data were collected in the trace-element geochemistry laboratory at Washington University, St. Louis, MO, using methods described in Korotev (1991). Various laminae within the calcretes were hand separated for analysis, to include samples with a range of detritus abundances. Splits of the other soils, of Unit 1 and Unit 2 (Table 1), as well as the eolian materials from above the soil horizons, were sieved into

coarse (<425 μm) and fine (<45 μm) fractions for analysis. Bulk samples of the soils and eolian materials were also processed for clay separation. Clay separates were obtained by shatterbox treatment, using W-carbide crushing elements, followed by sonic disruption in deionized water and separation of fine size fractions by settling or centrifugation. No chemical separations to remove carbonate or soluble Fe were used. Although some amorphous transition-metal deposits may be associated with the clays, it was the intent of this study to disturb the composition of the clay size fraction as little as possible. Clay fractions obtained were <3.0 μm; in some cases finer fractions (<1 μm) were separated as well. The INAA analyses of coarser and finer clay fractions show little chemical difference, although the purity of the coarser fractions was generally poorer. Mica remnants are generally more evident in powder X-ray diffraction (XRD) data collected from the coarser clay fractions (Fig. 2). The XRD analyses of clay separates were obtained with a Siemens D-500 diffractometer using Cu-Kα radiation and a Kevex Psi Si(Li) solid state detector. Quantitative XRD (QXRD) was performed with the same instrument, using sample portions mixed with a 1.0-μm corundum internal standard in a sample:corundum ratio of 8:2 by weight. The quantitative mineralogy was determined by the methods of Chung (1974). Further details of these methods can be found in Bish and Chipera (1989, 1991). Chemical analyses of Fe,Ti-oxide grains (principally hematites but including ilmenites, spinels, and rutile), biotites and other micas, and amphiboles were obtained from thin sections by electron probe microanalyis (EPM), using a Cameca SX-50 electron microprobe operated at 15 kV and 15 na sample current.

RESULTS

Over 350 analyses of Fe-rich detrital minerals (Fe,Ti-oxides, biotite, and amphibole) were obtained by EPM. Representative compositions of these three mineral types, from both the local tuffs and from the soils, are listed in Table 2. Both chemical data and optical character help to distinguish between minerals of different sources. The dominant local tuff is the densely-welded and devitrified rhyolitic portion of the Tiva Canyon Tuff, which contains about 3% phenocrysts, principally of sanidine plus a small amount (<0.1%) of amphibole and biotite. Titanomagnetite and ilmenite microphenocrysts, sphene, zircon, and small groundmass hematite and rutile grains are rare. Larger quantities of feldspar plus quartz phenocrysts (up to 15%), and amphibole plus biotite phenocrysts (about 0.6%) with trace amounts of clinopyroxene phenocrysts, are found in the upper quartz-latitic portion of the Tiva Canyon Tuff, but outcrops of this more mafic portion are poorly represented at the site. Moreover, the biotite and amphibole phenocrysts in these devitrified tuffs have been severely altered by oxidizing vapors during the cooling that followed ash-flow emplacement. As a result, both of these minerals in the devitrified tuffs are nearly opaque or have distinctive dark pleochroic colors (α = yellow, $\beta = \gamma$ = dark red-orange in amphibole; α = red-brown, $\beta = \gamma$ = dark red-brown in biotite). These colors are clearly distinctive in thin section and grains of this type are extremely rare in all of the soils and the eolian deposits. However, nonwelded portions of the Tiva Canyon and related tuffs occur in the region and may have provided unoxidized biotites and amphiboles that were transported to Exile Hill from localities within a few kilometers. Because of this possibility, it is necessary to rely

on chemical parameters to distinguish those biotites and amphiboles that are clearly exotic to the site. Chemical parameters can also be used in distinguishing exotic Fe,Ti-oxides that are not from tuffs at the site. Chemical parameters specific to each of these mineral types are described below, along with physical and optical descriptions of the principal features noted in thin sections of the eolian and soil deposits.

Fe,Ti-oxides; Hematite

Fe,Ti-oxide grains in the soils and eolian deposits are subequant and typically ~20 to 70 μm in diameter. Abundances are 1% or less. EPM shows that these grains represent both the ilmenite-hematite and magnetite-ulvöspinel compositional series, as well as some rutile. In contrast, the EPM data from tuffs show that the predominant oxide mineral in the tuff matrix, in both the quartz latites and rhyolites, is a high-Mn hematite. None of the Fe,Ti-oxides analyzed in soils and few in the eolian deposits have MnO contents >4% and none of the Mn-hematites analyzed from the tuffs have MnO contents <5%.

Biotite

Biotite grains in the soils and eolian deposits are variable in size, color, and extent of alteration. Small amounts of muscovite and chlorite are also found, but are much rarer than the almost pervasive biotites, which constitute 2% to 4% of these deposits. Typical biotite sizes are about 7x70 μm; only coarse grains (>10 μm) could be analyzed by EPM, but a large size range is present, with biotite fragments diminishing in dimension until

they approach the clay size fraction. Pleochroism of the typical soil and eolian biotites (α = pale yellow, $\beta = \gamma$ = yellow-green to orange) is much lighter than seen in biotites of the devitrified tuffs. The typical soil and eolian biotites have lower F contents and lower TiO_2/FeO ratios than the biotites in the tuffs.

Amphibole

Amphibole grains form 1-2% of the soil and eolian deposits and are typically 25 to 60 μm in size. As with the biotites, the amphibole grains have much paler pleochroism (α = pale yellow, β = pale green, γ = dark green) than the amphiboles in the tuffs. The amphiboles in the soils have generally higher FeO content (>14.5%) than the amphiboles in the tuffs (9% to 14.5% FeO).

Smectites

Smectites of the soils and eolian deposits are not analyzable by EPM, but XRD and INAA analyses provide considerable information about these clays in the eolian and soil deposits. Although of lower FeO content (~4.5-6%) than the hematite (80% FeO), biotite (14% FeO), and amphibole (15% FeO), the smectites are more abundant than these other minerals in the coarse A-horizon, B-horizon, and eolian deposits (12 ± 3 % smectite, versus <1 % for hematite, 3 ± 2 % for biotite, and 1 ± 0.5 % for amphibole). Distinct remnants of mica are observed in XRD analyses of the 3.0-1.0 μm clay size fraction (Fig. 2). These mica remnants are common to all of the eolian and soil smectites. Based on the high FeO contents of the smectites and on their association with very small

grains of biotite, this remnant mica is likely to be predominantly biotite. It is notable that the mica remnants are not a significant constituent in the finest clay fractions (<0.35 μm; Fig. 2), suggesting a lower size limit of ~1-0.35 μm for the mica component interposed with the poorly-crystalline smectite.

Table 3 lists the FeO, Sc, and lanthanide abundances in representative smectite separates from the eolian and soil deposits. The data in this table indicate a strong correlation between FeO and Sc contents but no apparent correlation between either of these elements and the lanthanide-element contents. The purity of the clay separates (weight percent smectite determined by QXRD) is indicated, ranging from 81% to 97%. Impurities in the clays are principally feldspar, silica minerals, and calcite, all of which have little impact on the measured FeO and Sc contents, and, in such small amounts, little effect on the lanthanide-element composition.

DISCUSSION

The optical and EPM data for hematites, biotites, and amphiboles indicate that derivation of these minerals from the local devitrified tuffs is not a significant factor in contributing Fe to the soils (Table 4). The mineral-chemical parameters on which a tuffaceous origin is assigned exclude virtually all hematites, most biotites, and about half of the amphiboles from being derived locally. Clearly, most of these silt-sized mineral carriers of Fe are of distant origin. The surprisingly high incidence of Mn-rich hematites of probable local origin in the eolian deposits (~25% of the hematites in these deposits)

may indicate that the collection of eolian materials from natural dust traps on tuff outcrops is subject to local contamination. Alternatively, the appearance of local hematites in these probably young eolian materials may indicate recent differences in eolian sources. Anthropogenic activity in historic times, particularly in the creation and use of dirt roads near Exile Hill, may be a significant factor in adding silt from local tuffs to the eolian deposits.

If the silt-sized Fe-rich mineral fraction in the eolian and soil deposits is mostly exotic in origin, then it should be expected that the smectite fraction would also be exotic. Figures 3 and 4 provide evidence that this is indeed the case. Figure 3 illustrates the strong correlation between Sc and FeO that is defined by the detritus in the calcretes [Sc (μg/g) = 2.33 x FeO (%); $r^2 > 0.99$]. The coarse Av, Btk, and 2Btj deposits were not used to define this regression line but clearly fall along it, indicating that detritus from the upper soil horizons defines the Sc/FeO ratio in the calcretes. This detritus includes a large proportion of eolian material (Table 4), but may also incorporate a lesser proportion of local tuff detritus with similar Sc/FeO ratios (Fig. 3). Vaniman et al. (1994, 1995) emphasize that the only local tuff with a Sc/FeO ratio that falls along this trend is an altered portion of the Tiva Canyon tuff that occurs at Exile Hill.

The coarse eolian deposits deviate slightly from the soil Sc/FeO ratio, perhaps for reasons of substrate contamination or anthropogenic modification of dust sources as previously discussed. More distinct is the different correlation between Sc and FeO in the clay separates from the eolian and soil deposits. This separate trend [Sc (μg/g) = 2.89 x FeO (%); $r^2 > 0.98$] represents the characteristic Sc/FeO composition of the exotic mica

component that has been contributed to the site by eolian sources over the past ~60 ka. Further evidence that this exotic mica component is the progenitor of eolian and soil smectite compositions can be seen in the comparison of smectite compositions derived by alteration of the local tuffs (Fig. 3). Smectites formed by tuff alteration have distinctly lower FeO content and have highly variable Sc/FeO ratios, with a higher Sc/FeO compositional range than their parent tuffs. These differences reflect the very different conditions that govern alteration of glassy tuffs in the subsurface, contrasted with smectite development from fine eolian materials that are dominated by mica rather than glass. Alteration of tuff glass produces smectites with no FeO enrichment over the source glass but with variably increased Sc content. Variability in Sc content of alteration smectites can arise from a number of causes, including temperature and fluid composition at the time of alteration, that are not as significant in surface weathering.

The two different Sc/FeO ratios shown in Fig. 3, derived separately from the calcretes and the eolian clays, both have zero intercepts within the errors of the linear fits to the data. This strongly indicates that the Fe-rich constituents, whether eolian minerals or local detritus, act simply as diluents in the manner in which they are added to local soils. Because the fine soil fraction (<45 μm) falls between the two regression lines, it appears that this fraction, which includes the largest population of single crystals of Fe-rich minerals other clays, has a mixture of the clay-size and silt-size detritus that contributes to both the eolian and soil deposits. The coarse eolian deposits also appear to have mixed sources, although they fall closer to the Fe-smectite regression line. This is

in accord with the observation that smectite and biotite (which is partially altered to smectite) are the principal reservoirs for Fe in the eolian deposits.

Borchardt et al. (1971) found that young soils developed by weathering of Mazama vitric ash in eastern Oregon had the characteristic Sc/FeO ratio of the source rock, but they also showed that Fe and Sc were highest in the shallowest soil clays. This is not the case at Exile Hill, where Sc and Fe abundances do not vary systematically with soil age or depth and the Sc/FeO ratio in the soil clays is characteristic not of the local rocks but of clays with a significant eolian biotite component. These contrasting systems show that there is not a single model for Sc and Fe accumulation in soil clays. Eolian contributions and presence or absence of abundant glass are both factors, in addition to the soil-forming processes that are specific to the local environment.

Figure 4 looks at the smectite origins at Exile Hill in a different manner. Here the lanthanide element compositions of eolian and soil smectites analyzed for this study are compared with smectites derived from tuff alteration (Vaniman et al., 1997). The very limited variability in lanthanide-element composition of eolian and soil smectites contrasts greatly with the highly variable lanthanide-element compositions of smectites derived by alteration of rhyolitic and quartz-latitic tuffs. Clearly, the eolian and soil smectites represent a different and more highly-constrained origin than do the smectites derived by tuff alteration. This highly-constrained origin is not difficult to discern. The patterned field in the upper part of this figure shows the range of eolian and model upper-crust lanthanide compositions that define broad, average samples of most of the Earth's upper surface. This indicates that the smectite/biotite components in eolian and soil deposits at Exile Hill are a result of regional wind-driven sampling of a zone far beyond

the Yucca Mountain area. Smectite, the most mobile of Fe sources at this site, is thus "exotic" in the sense of being derived from distant sources, but is largely mundane in averaging-out the various lithologies of its source regions.

ACKNOWLEDGEMENTS

This work was supported by the Yucca Mountain Site Characterization Project, Los Alamos National Laboratory, as part of the Civilian Radioactive Waste Management Program of the U.S. Department of Energy. Supporting field work by G. Guthrie and R. Raymond and guidance from E. Taylor in sampling and understanding the soils of Exile Hill is greatly appreciated. Review comments by S. Levy, G. Borchardt, and an anonymous reviewer helped to improve the manuscript.

REFERENCES

Balsam, W. L. and Otto-Bliesner, B. L., 1995. Modern and last glacial maximum eolian sedimentation patterns in the Atlantic Ocean interpreted from sediment iron oxide content. Paleoceanography **10**:493-507.

Bish, D. L. and Chipera, S. J., 1989. Revised mineralogic summary of Yucca Mountain, Nevada. Los Alamos National Laboratory report LA-11497-MS, 68 pp.

Bish, D. L. and Chipera, S. J., 1991. Detection of trace amounts of erionite using X-ray powder diffraction: Erionite in tuffs of Yucca Mountain, Nevada, and central Turkey. Clays & Clay Minerals **39**:437-445.

Birkeland, P. W., 1984. *Soils and geomorphology*, Oxford Univ. Press, New york, 372 pp.

Borchardt, G. A., Harward, M. E., and Knox, E. G., 1971. Trace element concentration in amorphous clays of volcanic ash soils in Oregon. *Clays and Clay Min.* **19**, 375-382.

Chung, F. H., 1974. Quantitative determination of X-ray diffraction patterns of mixtures. I. Matrix-flushing method for quantitative multicomponent analysis: Journal of Applied Crystallography **7**:519-525.

DeBaar, H. J. W., DeJong, J. T. M., Bakker, D. C. E., Loscher, B. M., Veth, C., Bathman, U., and Smetacek, V., 1995. Importance of iron for plankton blooms and carbon-dioxide drawdown in the southern ocean. Nature **373**:412-415.

Gile, L. H., Peterson, F. F., and Grossman, R. B., 1966. Morphological and genetic sequences of carbonate accumulation in desert soils. Soil Science **101**:347-360.

Korotev, R. L., 1991. Chemical stratigraphy of two regolith cores from the Central Highlands of the Moon. In: V. L. Sharpton and G. Ryder (Editors), Proceedings of the 21st Lunar and Planetary Science Conference. Lunar and Planetary Institute, Houston, pp. 229-289.

Taylor, E. M. and Huckins, H. E., 1995. Lithology, fault displacement, and origin of secondary calcium carbonate and opaline silica at trenches 14 and on the Bow Ridge Fault at Exile Hill, Nye County, Nevada. U. S. Geol. Survey Open-File Rept. 93-477, 38 pp.

Taylor, S. R. and McLennan, S. M., 1988. The significance of the rare earth elements in geochemistry and cosmochemistry. Handbook on the Phys. And Chem. of Rare Earths, Vol II. (K. A. Gschneider, Jr. And L, Eyring, eds.), Chapter 79, 485-578.

Vaniman, D. T., Chipera, S. J., and Bish, D. L., 1994. Pedogenesis of siliceous calcretes at Yucca Mountain, Nevada. Geoderma **63**:1-17.

Vaniman, D. T., Chipera, S. J., and Bish, D. L., 1995. Petrography, mineralogy, and chemistry of calcite-silica deposits at Exile Hill, Nevada, in comparison with local spring deposits. Los Alamos Nat. Lab. Rept. LA-13096-MS, 70 pp.

Vaniman, D. T., Chipera, S. J., and Bish, D. L., 1997, Mineralogic and chemical analyses of Exploratory Studies Facility (ESF) and core calcites, opals, Mn-oxides, and clays. Report SP321CM4, Yucca Mountain Project, Las Vegas, Nevada, 50 pp.

Table 1: Summary Slope-Wash Alluvium Soil Stratigraphy at Exile Hill (from Taylor and Huckins, 1995)

Unit 1 (soft, mostly eolian)	**Av***	Silty sand, <5 to 10 cm
	Btk*	Silty sand, 10-60 cm
Unit 2 (2Btj has prismatic structure; 2B+K includes calcrete plates of underlying K horizons)	**2Btj***	Silty sand, 0-30 cm
	2B+K	Sandy silt, 0-15 cm
Unit 3 (abundant secondary calcite and opal)	**3Kmq1***	Silty sand, 0-50 cm; strongly indurated; platy fabric
	3Kmq2*	Sand to silty sand, 0-50 cm; strongly indurated; platy fabric
	3Kq	Silty sand, 0-50 cm; indurated but lacks platy fabric
	3Bkq1	Silty sand, 50-175 cm; soft, with cemented gravel stringers
	3Bkq2	Sand to silty sand, 0-60 cm; soft

*Units in bold type were sampled for this study. Nomenclature used by Taylor and Huckins, 1995, follows Birkeland, 1984.

Table 2: Representative Mineral Compositions in Tuffs compared with Exotic Minerals in Soils*

	hematite (local tuff)	hematite (2Btj horizon)	biotite (local tuff)	biotite (Av horizon)	amphibole (local tuff)	amphibole (Av horizon)
SiO_2	-	-	34.6	37.0	49.0	47.1
TiO_2	3.59	10.3	6.59	5.00	0.84	0.53
Al_2O_3	0.28	2.05	12.9	14.6	4.60	8.74
Fe as FeO	-	-	13.2	14.4	10.4	15.1
Fe as Fe_2O_3	88.4	85.1	-	-	-	-
MnO	6.04	1.25	1.23	0.24	2.34	0.29
MgO	0.89	1.09	18.3	15.2	16.2	13.2
CaO	-	-	0.29	0.03	9.64	12.3
Na_2O	-	-	0.99	0.58	3.63	1.23
K_2O	-	-	7.59	8.33	0.57	0.32
F	-	-	4.26	0.70	2.64	0.82
Σ	99.2	99.8	100.0	96.1	99.9	99.6

*all data in weight percent

Table 3: FeO, Sc, and Lanthanide Compositions of Soil Smectites

	eolian	Av horizon	Btk horizon	2Btj horizon
FeO (wt. %)	6.06	4.47	5.14	5.10
Sc (μg/g)	16.40	11.85	13.66	13.93
La (μg/g)	48.9	39.8	49.0	49.6
Ce (μg/g)	105.7	88.5	100.5	105.4
Nd (μg/g)	38	31	38	38
Sm (μg/g)	7.66	6.33	7.83	8.08
Eu (μg/g)	1.09	0.863	1.08	1.12
Tb (μg/g)	.95	0.82	0.96	1.09
Yb (μg/g)	2.97	2.83	3.26	3.65
Lu (μg/g)	0.432	0.426	0.486	0.535
purity of clay separate	*95%*	*81%*	*90%*	*97%*

Table 4: Identification of *Minimum* Proportion of Grains that are of Exotic Origin in Eolian and Soil Deposits at Exile Hill

mineral	proportion exotic	criteria used to determine exotic origin
hematite	100% (except eolian deposits, >75%)	MnO < 5%
biotite	>67%	TiO_2/FeO > 0.27; F < 1% at FeO > 15%
amphibole	>50%	FeO > 14.5%

Figure captions:

Fig. 1: Location map showing Exile Hill and the sample collection sites for eolian and soil materials. Eolian samples were collected from fissures in boulders at the locations marked ⊗. Soil B horizons and calcretes were sampled within trenches on the east and west slopes of Exile Hill (shaded locations). The soil A horizon was sampled at an undisturbed area (A) west of the ridge crest. Contour elevations are in meters.

Fig. 2: XRD patterns of two clay size fractions from the 2Btj horizon at Exile Hill. Symbols identify peaks for calcite (C), feldspar (F), kaolinite (K), mica (M), quartz (Q), smectite (S), and zeolite (Z). The 3.0-1.0 μm fraction consists of 76% clay plus mica and 20% feldspar plus quartz, with 4% consisting of the remaining minerals. The 0.35-0.10 μm fraction consists of 97% clay (with very little mica) and 3% calcite. Percentages cited are weight proportions determined by QXRD.

Fig. 3: Distinctive Sc/FeO ratio of calcretes at Exile Hill, contrasted with the smectites in eolian deposits and soil A and B horizons. These surficial materials fall along or (for coarse eolian deposits) between two different regression lines. The lower regression line

is defined by coarser detritus in the calcretes with an appreciable local tuff component as well as eolian contributions. The upper regression line is defined by Fe-rich eolian micas. The ranges of compositions for local tuffs and for smectites derived by alteration of those tuffs are also shown.

Fig. 4: Comparative chondrite normalized lanthanide-element plots of (a) eolian and soil smectites and (b) smectites derived by subsurface alteration of local tuffs. Shaded pattern represents global loess and model upper-crust compositions (Taylor and McLennan, 1988). The 7 eolian and soil smectites from Exile Hill plotted in (a) have a narrow range of compositions that is similar to eolian materials representing areal averages of large tracts of crustal material. The 15 smectites in panel (b), derived by subsurface alteration of local tuffs, have widely varying compositions; high lanthanide contents with little or no Eu anomaly reflect alteration of local quartz-latitic tuffs and lower lanthanide contents with appreciable negative Eu anomalies reflect alteration of rhyolitic tuffs.

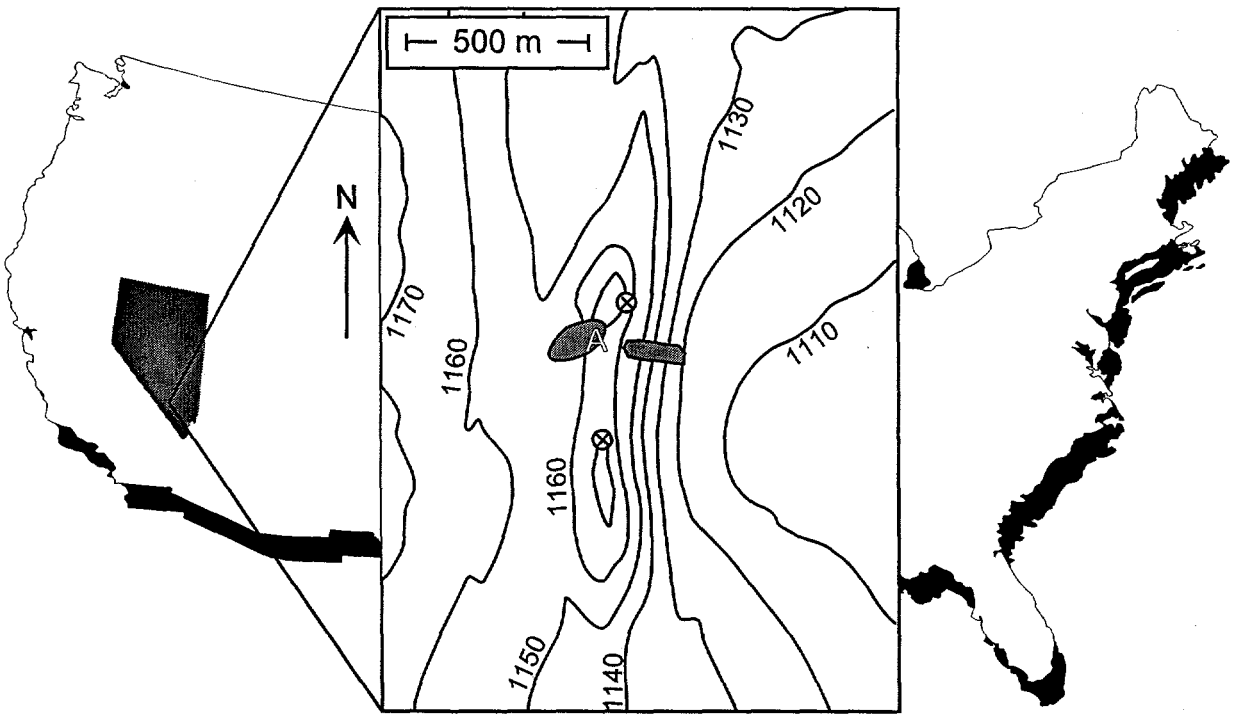

Figure 1
Vaniman et al.

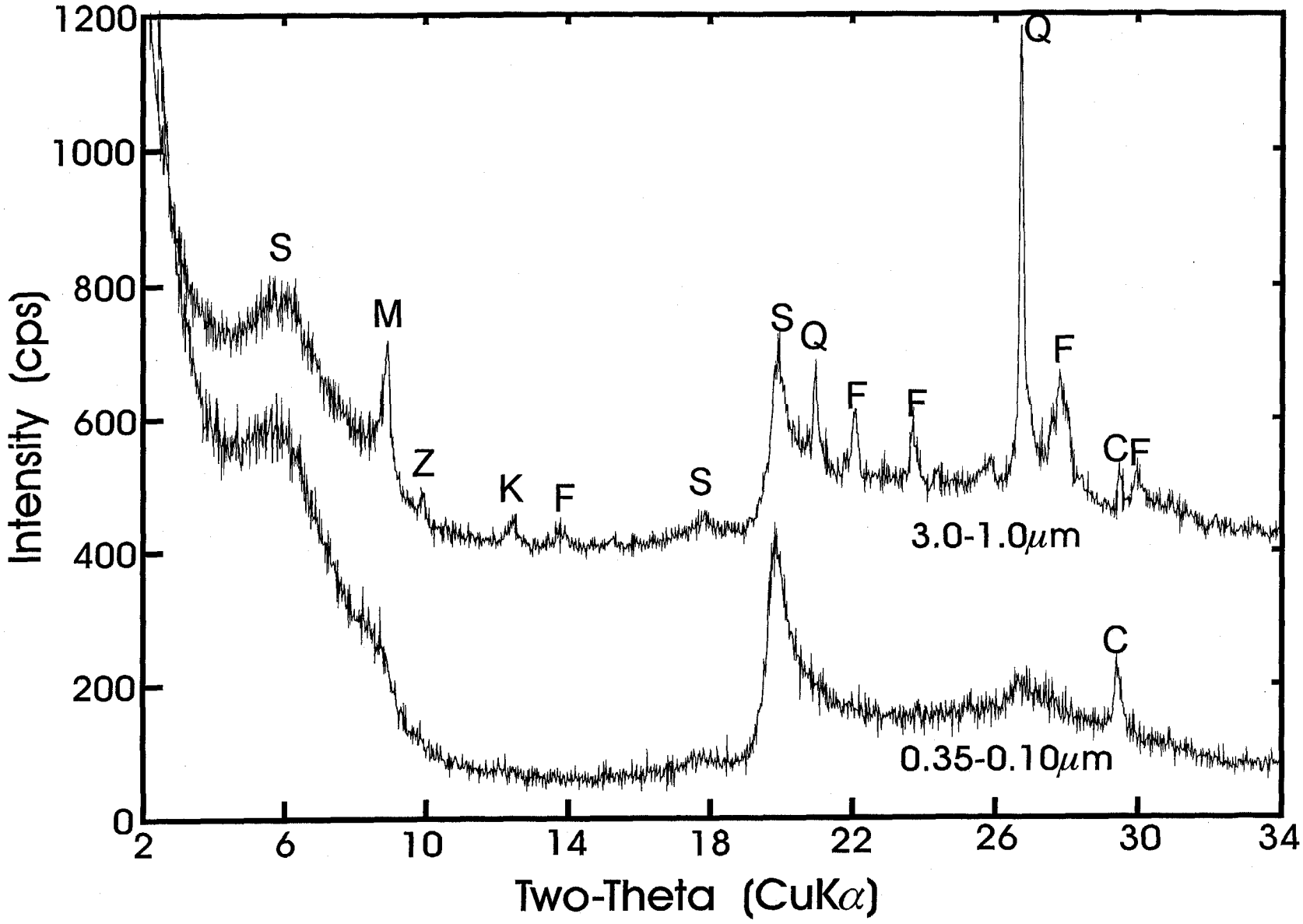

Figure 2
Vaniman et al.

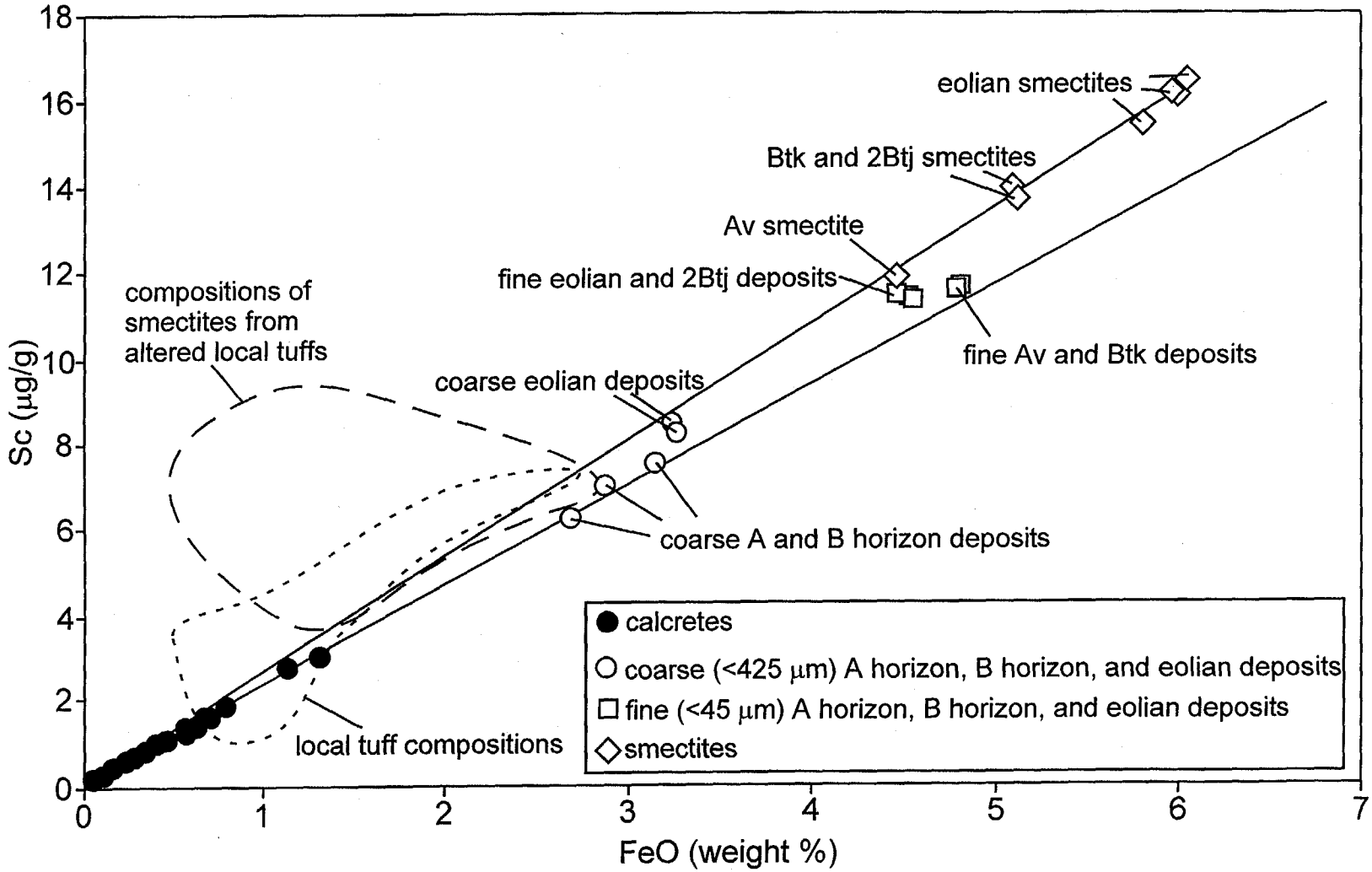

Figure 3
Vaniman et al.

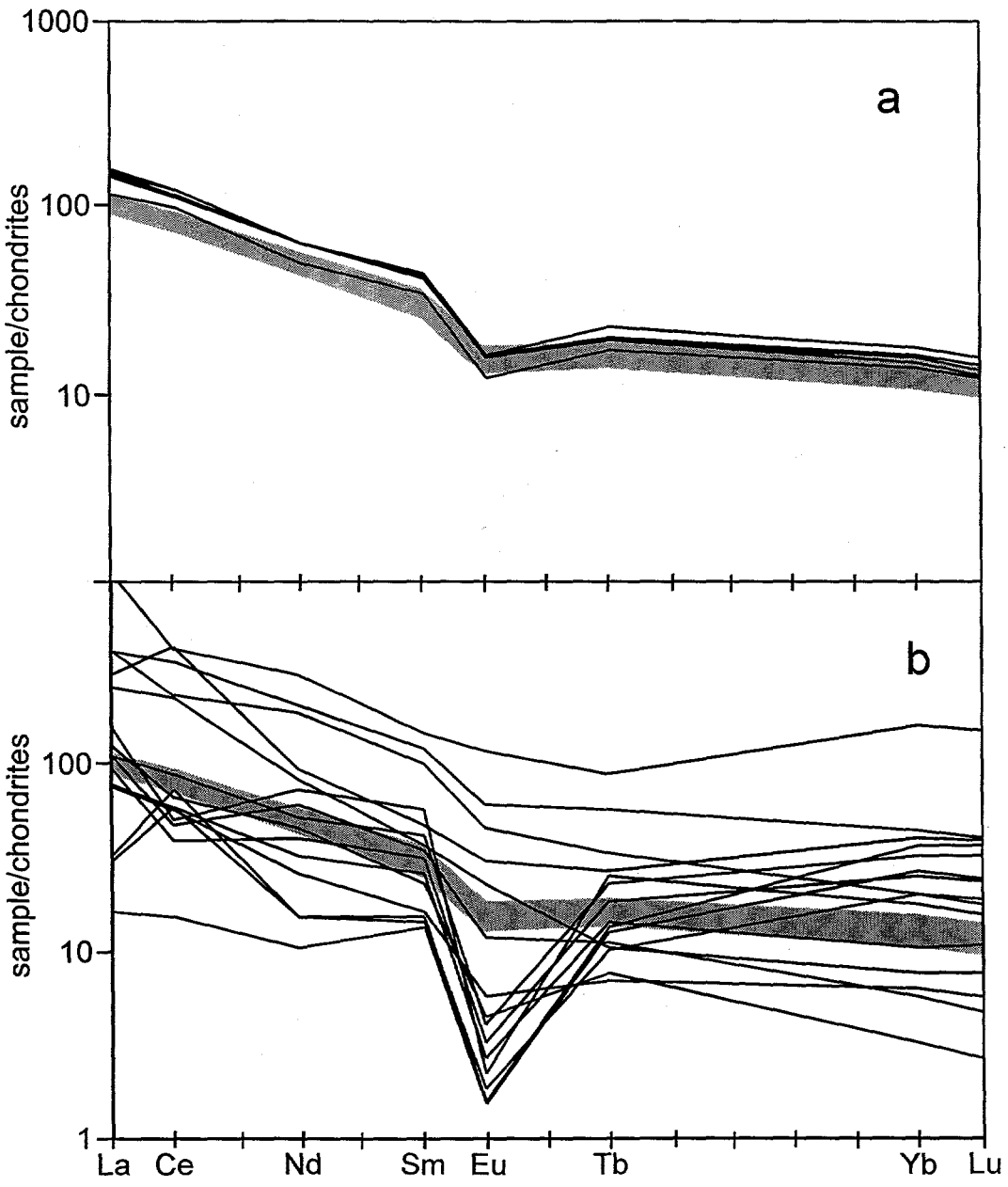

Figure 4
Vaniman et al.